THE PENNSYLVANIA STATE UNIVERSITY
SCHREYER HONORS COLLEGE

DEPARTMENT OF MATERIALS SCIENCE AND ENGINEERING

MICROMAGNETIC SIMULATIONS OF CoPt: INVESTIGATION OF DOMAIN WALL PINNING

ZACH JOHNSON
Spring 2013

A thesis
submitted in partial fulfillment
of the requirements
for a baccalaureate degree
in Materials Science and Engineering
with honors in Materials Science and Engineering

Reviewed and approved* by the following:

Roman Engel-Herbert
Assistant Professor of Materials Science and Engineering
Thesis Supervisor

Allen Kimel
Assistant Professor of Materials Science and Engineering;
Associate Head for Undergraduate Studies
Honors Adviser

* Signatures are on file in the Schreyer Honors College.

ABSTRACT

This thesis presents results for the micromagnetic simulation investigation of domain wall pinning in the material system CoPt. Defect sites were modeled as areas with a higher anisotropy than the rest of the CoPt in order to create an area resistant to a change in magnetization. Domain wall displacement was studied as a function of defect pinning strength and defect pinning distance. It was found that as the defect distance increases, the domain wall becomes "looser" and propagates through the material system further at the same value of external magnetic field. Furthermore, the energy contributions to the magnetic system were investigated in order to explain the nature of the propagation of the domain wall movement. Finally, a study of anisotropy energy as a function of domain wall displacement is presented, in order to correlate the energy of the magnetic system directly to the distance that a domain wall is displaced. In this way, it would be possible to predict the domain wall displacement of a material system, if the energies of the system are known.

TABLE OF CONTENTS

LIST OF FIGURES

ACKNOWLEDGEMENTS

I would like to express my gratitude to my family, for always supporting me. They have always been there for me when I am struggling. This thesis was no different – my family always kept me motivated and positive. I would also like to thank my advisor, Roman Engel-Herbert, for working with me on this project. I learned a great deal from him about research, problem solving, and critical thinking.

Chapter 1

Introduction

History of Magnetic Memory

Magnetic materials are becoming increasingly important for today's memory applications. Magnetic memory storage began with the replacement of the punch card with magnetic tape [1]. Punch cards use physical holes to store data that a computer can read. The data density is very low, since the holes are physically large. The introduction of magnetic tape drastically increased the data density by storing data within magnetic domains, and then having a device read the domain orientation [1].

Magnetic materials revolutionized the music industry. Vinyl records were replaced by cassette tapes, which make use of magnetic tape to store musical data [2]. Vinyl records were very large, and somewhat immobile, but the introduction of cassette tapes brought music into a compact and portable format. They were hugely popular, as the average person could now listen to cassettes in the car, or with a Walkman (a portable cassette player).

Computers began using hard disk drives to store data [3]. Each bit of data is stored in a magnetic domain that is aligned either up or down. Whether the domain is up or down determines whether the computer reads the domain as a 1 or a 0. The arrangement of the magnetic domains forms a set of data or a calculation for the computer to read. The magnetic domains are read by a magnetic sensor.

Initial versions of magnetic sensors use the anisotropic magnetoresistance effect to read magnetic domains. Spin-valve sensors replaced these old sensors with the discovery of the giant magnetoresistance effect. Spin-valve sensors have two different materials layered on top of one

another. One has a small magnetic coercivity (the strength with which the material will hold its current magnetization), while one has a high magnetic coercivity. When the two magnetic materials are aligned in the same direction, the electrical resistance across them is low, and when the two magnetic materials are aligned antiparallel, the electrical resistance across them is high. When this sensor is passed over a magnetic domain, the material with the small magnetic coercivity will take on whichever orientation the magnetic domain currently holds. This changes the resistance of the spin-valve sensor, and allows reading of magnetic domains. Figure 1-1 shows how the resistance changes with the orientation of the low coercivity material. Spin-valve sensors increased sensitivity, and this enabled scaling of magnetic memory.

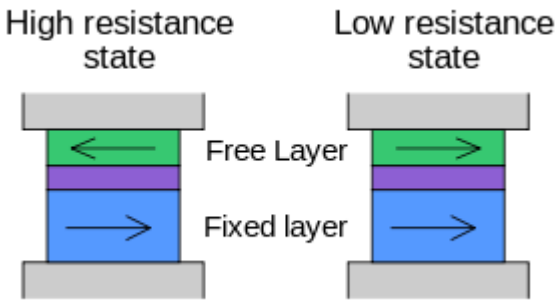

Figure 1-1. Spin-valve sensor. Two magnetic materials operate in conjunction with one another to change the resistance between them so that magnetic domains can be read (Figure reproduced from Wikipedia.com)

A problem arises with magnetic memory storage like this, though. The magnetic domains have to be read by a sensor, and a data stream can only be read if the sensor is moved across the magnetic material. Cassette tapes solve this issue by using a motor to move the magnetic tape, while the sensor remains stationary. Computer hard disks move the sensor to different regions of the magnetic disk. In both cases, large mechanical movements are required, which ultimately limits the scaling of such devices. It would be superior to be able to move the magnetic domain

structure itself, rather than a physical object, in order to reduce the mechanical movement required, which would enable the continuation of scaling.

Racetrack memory, being developed by IBM, introduces a new, fast way to store data. Racetrack memory makes use of magnetic domains within nanowires. When a current is passed through the nanowire, the entire magnetic structure is moved along the nanowire. The wire is in a U shape, and at the bottom of the U, a pair of devices reads the magnetic domains passing by. The domains move very quickly upon application of a current, making racetrack memory fast. With enough wires, and enough bits stored on each wire, the data density and speed of racetrack memory can exceed current memory technologies [4]. There is no mechanical movement involved in racetrack memory, mean which means that racetrack memory can be performed on a nano-scale. Figure 1-2 illustrates a racetrack memory nanowire with a positive and negative current.

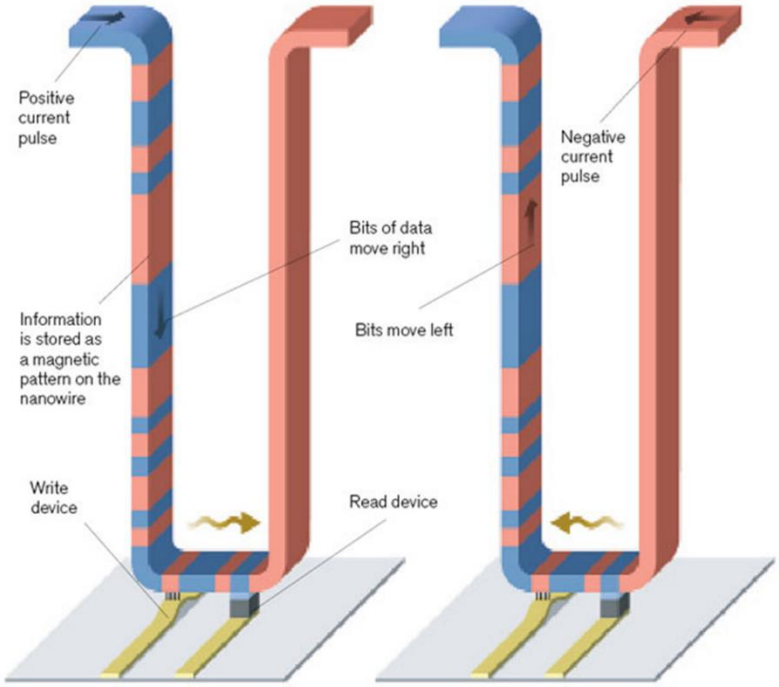

Figure 1-2. Racetrack memory wire. Shown with positive current and negative current. (Figure reproduced from IBM)

Understanding the mechanisms governing domain wall movement is key for proper implementation of racetrack memory. Material defects can impair domain wall movement, pinning the domain wall in the area of the defect, while the rest of the wall bulges outward, like a rubber band being stretched. Research innovations like racetrack memory introduce a need for greater understanding of magnetic domain dynamics in wires. There are two ways that magnetic domains can be moved within a wire: current and magnetic field. Experiments in conjunction with simulations at the proper length scale of magnetic domains is need to better understand how domains propagate through a wire. The length scales range from a few nanometers up to a few micrometers. Micromagnetic simulations use a mean field approach. The total energy of the system is assumed to depend only on the magnetization of the material, or the magnetic domain arrangement.

Performing experiments on various materials to study domain wall movement is costly and time consuming. However, micromagnetic simulations offer a highly controlled environment in which to study a material's magnetic responses in a costly fashion. The only resource being consumed is the energy required to power the computations. Micromagnetic simulations enable tuning of different material properties, control over external magnetic fields and internal currents, and sample dimensions. They provide both numerical and visual results, making the simulations intuitive to understand.

Motivation

The motion of domains and domain walls in magnetic materials brings up several interesting questions. How can we reproducibly displace domains without changing them, and how can we do it quickly? Material defects present issues with reproducibility and speed – they can impair movement of the domain structure, and possibly change it. As magnetic wires get

smaller, material defects present more of an issue. It is essential that the relationship between material defects and domain wall propagation is well understood. Current micromagnetic simulation packages offer the ability to model defect sites and pinning centers. However, not much work has been done in this area.

The goal of this thesis is two part. First, to determine a way to model defect sites in an accurate matter. Second, to further investigate domain wall pinning in CoPt, by changing pinning strength, distance between defects, energy damping, and stepping size. First, an introduction to the theory of micromagnetics and the equations behind micromagnetic simulations is presented. Background information on the material system CoPt is presented. Second, a description of domain wall flexing in CoPt is discussed with respect to material defects. The results are summarized, and possible directions for future work are given.

Chapter 2

Basics of Micromagnetic Simulations

Magnetism is inherently quantum mechanical in nature. The magnetic moment of an atom is given by

$$\mu = -g\mu_B(L + S) \tag{2.1}$$

where μ is the magnetic moment, g is the Landé factor, μ_B the Bohr magneton, L the orbital momentum, and S the electron spin. The total energy of interacting magnetic moments have four contributions: Zeeman energy, anisotropy energy, exchange field energy, and stray field energy. Detailed descriptions of these energy terms is given below. All these energy terms depend on the geometric arrangement of these magnetic moments, represented by the magnetization of the material. The magnetization, $\vec{M}(\vec{r}, t)$, is a vector quantity that represents the direction of magnetization as a function of time and position. Where μ is the magnetic moment of an individual atom, $\vec{M}(\vec{r}, t)$ is the field mean of these individual magnetic moments. The magnitude of the magnetization is the saturation magnetization M_s which is assumed to be constant throughout the material. The micromagnetic simulation program now calculates these energy terms and seeks to minimize the total energy in the system. It is assumed that the magnetization $\vec{M}(\vec{r}, t)$ with the minimum total energy is the physically correct magnetic domain structure. Thus, from an assumed starting magnetization the micromagnetic simulator can determine the correct magnetic domain structure by evolving the given magnetization towards the equilibrium state.

A micromagnetic simulator cannot, however, model each individual magnetic moment for each atom. Instead, a cell size is defined, and a magnetic moment is assigned to each cell.

Cells then populate a mesh in a defined geometry to create the desired material. When the simulator calculates the energy of the system, it has to compare each magnetic moment to every other magnetic moment. So, the smaller the cell size, the more computational time the simulation will take, but the more realistic the simulation will be. Too large of a cell size can introduce systematic errors into the simulation. A cell size of 5x5x5 nm was used for all simulations. Assuming an atomic radius of 1.5 Angstrom, this cell size comprises about 1700 magnetic moments from individual atoms. This gives a simulation that is accurate, but still computationally reasonable.

Magnetic Energy Terms

The following energy terms represent energy densities. The maximum energy of the system is given by $\frac{\mu_0}{2} M_s^2$. This maximum energy will be used later on to compare various energy terms to a standard value.

Zeeman Energy

The Zeeman energy relates the magnetic moments in a material to an external applied magnetic field. The Zeeman energy of a single magnetic moment is given by:

$$\varepsilon_{Ze}^{i} = -\mu_o \mu_i \cdot H_i \qquad (2.2)$$

where μ_0 is the permittivity of free space, μ_i is the magnetic moment in question, and H_i is the applied external magnetic field. The Zeeman energy is minimized when all magnetic moments are aligned parallel with the applied field or antiparallel with the applied field. If magnetic moments are not aligned with the external magnetic field a torque will act on the

magnetic moment that will align the magnetic moment with the field. The torque is given by the vector product between magnetic moment and applied field. The problem in micromagnetic simulations is that if there is ideal antiparallel alignment of a magnetic moment with the external field, the torque is zero and the moment cannot be aligned with the external field direction. This can cause issues in the simulation data, because although it seems like a material's magnetic moments should be switching, they will not if the applied field is perfectly antiparallel to the direction of the magnetic moments. To solve this issue, the applied magnetic field must be offset slightly in one direction to break the symmetry of the problem. This equation can be summed over the entire area of the sample for each magnetic moment to obtain a total Zeeman energy for the system.

Demagnetization Energy

A ferromagnetic material has a spontaneous magnetization associated with it, which creates a magnetic field. This magnetic field is often times called the stray field or fringe field that interacts with the magnetization of the material giving rise to the self-energy. The stray field increases as the magnetization in the sample increases, and decreases as the magnetization decreases. So, the stray field attempts to demagnetize the material in order to minimize energy. Thus this energy contribution is called the demagnetization energy. The stray field energy is given by:

$$\varepsilon_{sf} = -\frac{1}{2}\int_{sample} \vec{H}_D \cdot \vec{\mu} dV \qquad (2.3)$$

where H_D is the field generated by the sample, μ is a magnetic moment, and the integral sums up each interaction through the volume of the sample [5]. Figure 2.1 shows the effects of stray field energy [6].

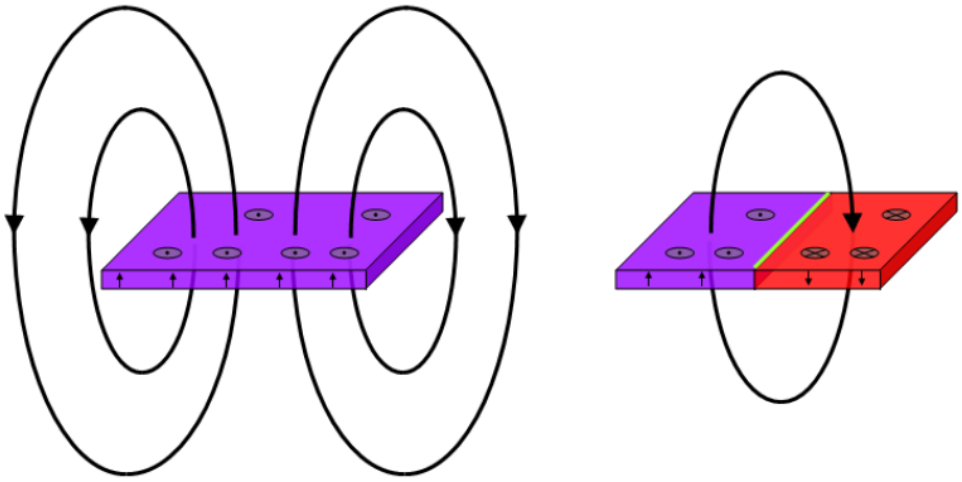

Figure 2-1. Demagnetization energy. On the left is a material with magnetization all in one direction, giving high energy. Demagnetization acts to minimize energy in the system, resulting in the material on the right.

Anisotropy Energy

In the case of magnetic energy, it follows that anisotropy energy is an energy than changes bases on the particular direction a magnetic moment is pointing within a crystal lattice. Depending on the material, certain crystallographic directions will have lower or higher energies than other directions. This arises from spin-orbit coupling and the strength of the anisotropy. The energetically preferred directions are thus material specific. Anisotropy reflects the symmetry of the magnetic material. For example if a crystal has one direction of preferred magnetic moment orientation, then it has uniaxial anisotropy. If it has more than one preferred magnetic moment

orientation, then it is deemed cubic anisotropy. A preferred crystallographic direction is termed an easy axis, while the energetically disfavored direction is called a hard axis. The anisotropy energy is at a minimum when all magnetic moments in a sample are aligned in one of the preferred crystallographic directions. The anisotropy energy increases as the angle between the magnetic moment and the preferred direction increases, and reaches a maximum at 90°. The simulations presented in this these focus on CoPt, which has a uniaxial anisotropy along the (001) direction. The uniaxial anisotropy is given by:

$$\varepsilon_{Ani} = K_u \sin^2\theta \tag{2.4}$$

where K_u is uniaxial anisotropy constant and Θ is the angle between the direction of the magnetic moment and the easy axis. This anisotropy energy has to be calculated for each magnetic moment in the sample, and then can be summed across the sample to yield a total anisotropy. Figure 2.2 shows a mesh of the anisotropy energy for iron and nickel, two common magnetic materials [6]. The anisotropy of the two materials is vastly different.

In addition to the bulk anisotropy effect, there is also surface and interfacial anisotropy. This exists because of the difference in bonding in these two cases. Interfacial anisotropy plays an important role in CoPt, because it allows an out of plane magnetization to be possible.

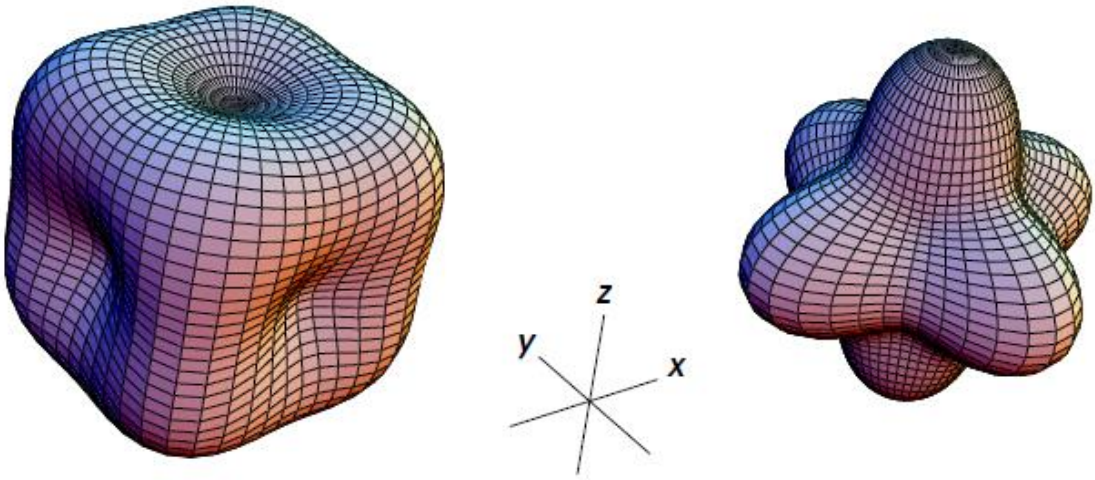

Figure 2-2. Anisotropy energy for two materials. On the left is the anisotropy energy for iron, and on the right, the anisotropy energy for nickel. The two materials have maximum anisotropy energy along different crystallographic directions.

Exchange Energy

The exchange energy is the energy associated with the interactions of magnetic dipoles with one another. It is purely quantum mechanical arising from the exchange interaction of magnetic moments at neighboring lattice sites and only acts on short length scales. In a ferromagnetic material, magnetic dipoles seek to align with one another. The exchange energy is minimal when all dipoles are aligned in the same direction. The exchange energy between two magnetic moments is given by:

$$\varepsilon_{ex}^{ij} = -\mathrm{J}S_i \cdot S_j \tag{2.5}$$

where ε_{ex} is the exchange energy, S is the unit vector of a magnetic moment, i and j denote two magnetic moments [7]. J is the exchange integral and it comes from wave function interactions between two electrons. J can be determined both experimentally and from density functional

theory and varies from material to material. The exchange energy for a system of particles is given by:

$$\varepsilon_{ex} = \frac{1}{2}\sum_{i}\sum_{j\in N_i} \varepsilon^{ij} \tag{2.6}$$

where N_i signifies the nearest neighbors.

The Equation of Motion

The equation of motion for a magnetic moment is given by:

$$\frac{d\boldsymbol{M}(\vec{r},\vec{t})}{dt} = \frac{\gamma}{1+\alpha^2}\boldsymbol{M}(\vec{r},\vec{t}) \text{ x } H_{eff}(\vec{r},\vec{t}) - \frac{\alpha\gamma}{1+\alpha^2 \cdot M_S}\boldsymbol{M}(\vec{r},\vec{t}) \text{ x } [\boldsymbol{M}(\vec{r},\vec{t}) \text{ x } H_{eff}(\vec{r},\vec{t})] \tag{2.7}$$

where γ = 2.21 · 105 m/A·s is the gyromagnetic ratio of the free electron spin, and alpha is a damping constant [5] [8]. The first and second terms in Eq. 2.7 describe the rotational progression of a magnetic moment around the effective field axis and the damping of the energy of the magnetic moment, respectively. α is a parameter that can be chosen within a micromagnetic simulation, typically between 0.01 and 1. As magnetic moments oscillate, α is the parameter that reduces the radius of the oscillation so that eventually they come to rest. A larger α will damp a magnetic moment faster than a small alpha, and the material will come to equilibrium faster with a larger alpha. A micromagnetic simulator uses Eq. 2.7 to evolve a system

towards equilibrium, so the choice of α is often not critical, since a larger α will result in a quicker simulation. Figure 2-3 shows the evolution of a magnetic moment with damping [5].

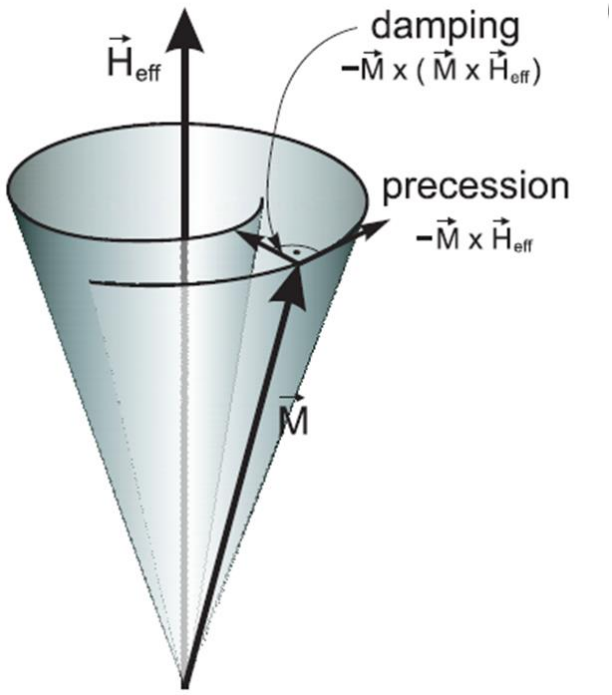

Figure 2-3. Progression of a magnetic moment with a damping constant, alpha.

Hysteresis

A hysteresis curve is an excellent starting place when investigating the magnetic properties of a material. Magnetic hysteresis means that the materials previous magnetic history influences its current magnetic state and progression towards a different magnetic state. It provides information about the anisotropy of a material (both direction and strength), saturation magnetization. Furthermore it provides the magnetic field strength needed to flip magnetic domains (coercive field) and the remnant magnetization in the absence of magnetic fields.

Therefore simulating hysteresis curves are important to determine if the simulation parameters used will reproduce magnetic properties of the material under study.

We have performed simulations of the hysteresis curve by first relaxing a material into an equilibrium state, with all of its domains pointed in one direction, with magnetism equal to the materials saturation magnetization. An external magnetic field is applied, starting at a small value with opposite sign to the current domain direction, and slowly ramping up in magnitude. At some value of the external magnetic field, the coercive field is reached, and the magnetic domains flip. It varies depending on how anisotropic the material is and the saturation magnetization of the material. For a highly anisotropic material, like CoPt, there will be very little variation in the magnetization of the material before or after the coercive field is reached. A hysteresis curve for CoPt is shown below in Figure 2-4.

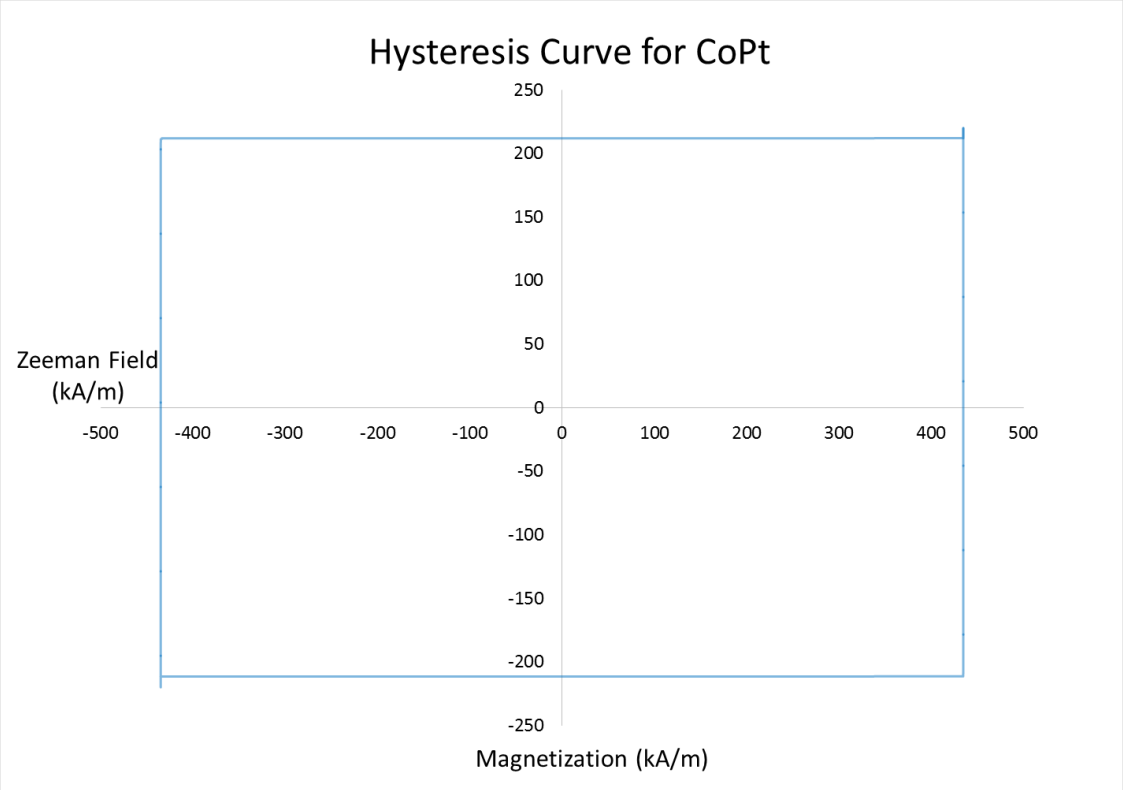

Figure 2-4. Hysteresis curve for CoPt. The highly anisotropic nature of CoPt gives the hysteresis curve very sharp changes in magnetization, rather than a gradual change that would be observed in a material with lower anisotropy.

The coercive field for CoPt occurs at 211.5 kA/m. However, this value changes slightly with two simulation parameters, alpha and step size. As stated earlier, alpha is a damping mechanism. This has important consequences when performing micromagnetic simulations. When a hysteresis simulation is executed, an external magnetic field is applied, and then the simulator "relaxes" the material to an equilibrium state, which will vary depending on what the current external field value is. A small alpha results in a longer computational time, since the system takes longer to reach equilibrium. However, a small alpha also results in a more accurate simulation, because a smaller alpha better approximates a real world material.

Step size also affects the coercive field value. Step size is the amount the external field is increased or decreased during the hysteresis simulation in between each relaxation of the material. A larger step size consequently gives a faster calculation of the hysteresis curve, but a more inaccurate one. A large step size may overshoot the coercive field, giving inaccurate results for the coercive field. A small step size will hone in on the exact coercive field, but it will also take significantly more computational time, since the simulator has to relax to an equilibrium state many more times.

An investigation of alpha and step size was performed in order to determine optimal values for each of them that give an accurate representation of the coercive field and a hysteresis curve, while still maintaining a reasonable computational time. Hysteresis simulations were performed for step sizes of 0.1, 0.5, 1, 5, and 10 kA/m, and for alpha values of 0.01, 0.02, 0.05, 0.1, 0.2 and 0.5. With an alpha of 0.01, simulations could take over 8 hours to run, but with an alpha of 0.5 simulations would take less an hour. Figures 2-5 shows a plot of coercive field versus alpha. It would be expected that as step size is decreased, the coercive field would decrease as well. This is due to the fact that a magnetic system should theoretically switch magnetization as soon as the coercive field is reached, so with a smaller step size, this will occur at a smaller value. However, Figure 2-5 shows that this is not always the case. As stepping of the external magnetic field gets smaller, there are deviations in the coercive field. These fluctuations are attributed to the relaxation criteria that the simulation uses to evolve at each step size. With large step sizes, there is a larger perturbation in the equilibrium of the system, so when the system increases the magnitude of the magnetic field, it will take longer to reach an equilibrium than in the case of smaller step sizes. In fact, with smaller step sizes, the system may actually not reach an equilibrium prior to moving on to the next step. If the magnetic field stepping is too small, the initial perturbation of the system may not be strong enough to drive the system far enough away from the equilibrium condition. The simulation will continue to the next field step, even though it

is possible that the coercive field had already been reached. Interestingly, the strange behavior is seen at lower step sizes and when the damping constant, alpha, is small. The reason for this is not clear, as it seems that a smaller alpha should always give a more accurate coercive field. An alpha of 0.2 was chosen for most simulations. This choice of alpha is adequately small so that the simulation is as accurate as possible, but keeps computational time at a minimum. The choice of step size for the hysteresis curve did not affect the step size used in future calculations, as the domain wall simulations require a different approach.

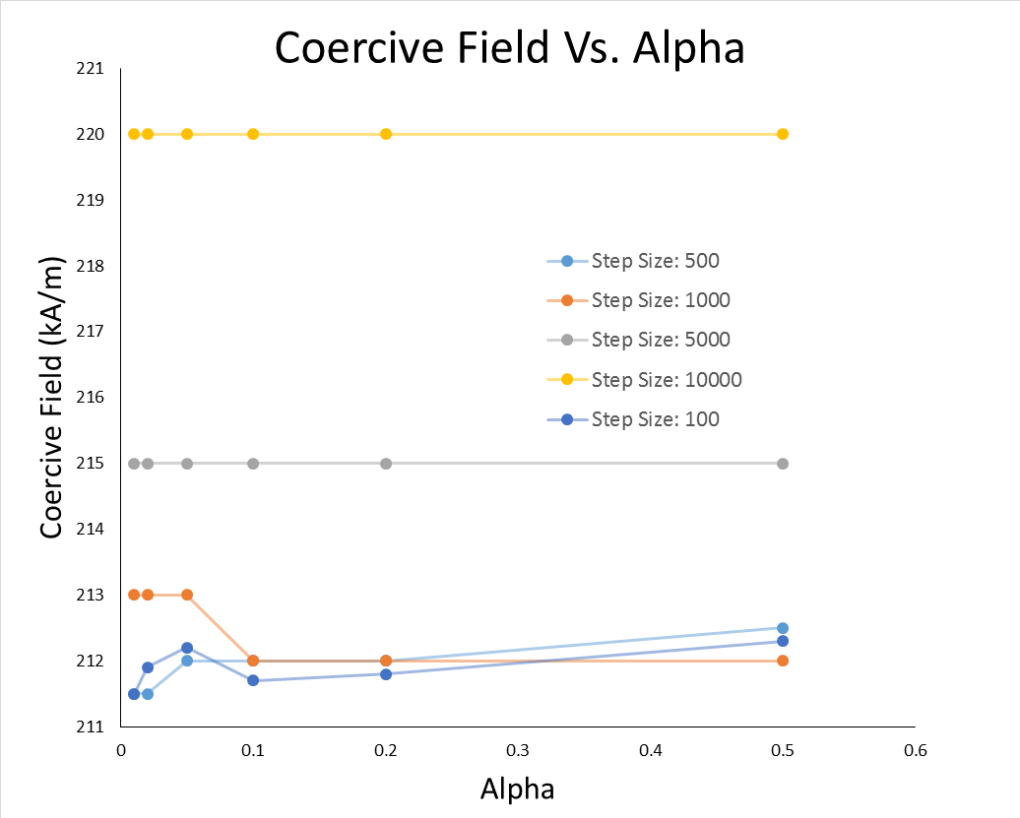

Figure 2-5. Coercive Field vs. Alpha. Strange trends are noticeable at low step size and low alpha

CoPt - Material Properties and Simulation Parameters

CoPt is a layered material, with out-of-plane magnetization. This is important for memory applications, such as racetrack memory, because out-of-plane magnetization allows nanowire domains to be structured so that they can be aligned either up or down, giving either a 1 or a 0 command. Cobalt on its own is a magnetic material with in-plane magnetization, and platinum is not magnetic at all. Interfacial interactions between cobalt and platinum change the preferred axis to be out of plane, rather than in plane.

CoPt alloys form a complete solid solution [9]. When the ratio is close to 50 : 50, CoPt is a permanent magnetic material, suitable for memory applications. Figure 2-6 shows the unit cell of a 50 : 50 CoPt alloy [10].

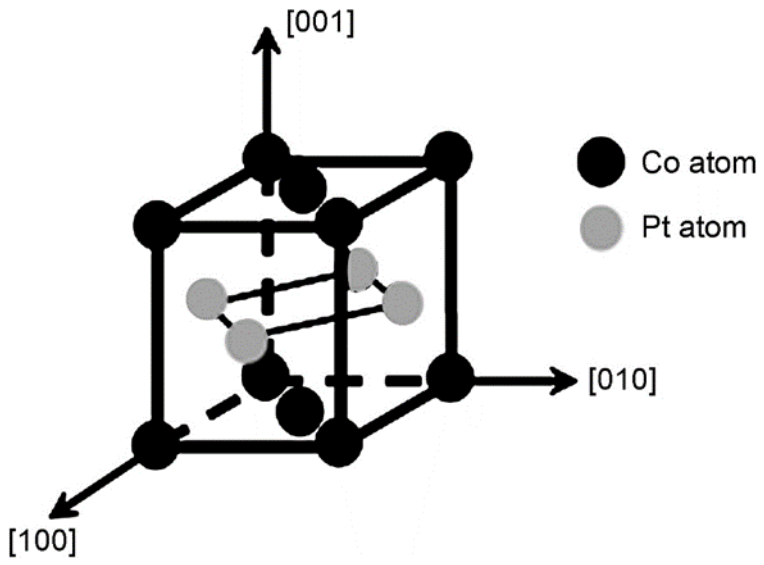

Figure 2-6. Unit cell for CoPt, showing a layered structure.

Several micromagnetic simulation parameters determine the magnetic material. Anisotropy axis, and magnetocrystalline anisotropy define the preferred magnetic orientation of the crystal, and how strongly it prefers that orientation, respectively. CoPt has an anisotropy axis of [001] and a magnetocrystalline anisotropy of 1.7×10^5 J/m^3. Exchange stiffness constant is a measure of how strongly two magnetic moments interact. CoPt has an exchange stiffness constant of 1×10^{-11} J/m Saturation magnetization (M_s) is the maximum magnetization that the magnetic material will experience. CoPt has an M_s of 435 kA/m, however this value can change slightly depending on temperature and composition of the alloy [9].

Chapter 3

Domain Wall Analysis

Modeling Pinning Sites

A hysteresis curve was calculated for CoPt, and it was consistent with the expected result for a highly anisotropic material: it had sharp edges, with a rapid change in magnetization at the coercive field. This result shows that the micromagnetic simulator is accurately portraying CoPt, and now the next step is to model defect pinning sites.

Defect pinning in domain wall motion was studied by setting up a simulation with a two micrometer long piece of CoPt. Two defect sites were midway along the length, at each side of the width. The width was varied between 500 nanometers and 1000 nanometers, in order to see the effects of distance between pinning sites. Figure 3-1 shows a two micrometer by 500 nanometer piece of CoPt, with two defect sites indicated by arrows. This image is taken prior to application of an external magnetic field.

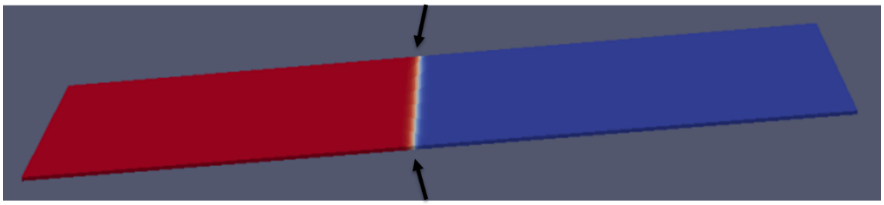

Figure 3-1. Starting configuration of a domain wall propagation simulation.

Defect sites were modeled as point defects with a higher anisotropy constant than the rest of the material. This creates a pinning field for the domain wall. When an external magnetic field is applied, one of the domains will be aligned parallel to this external field, and the other domain will be aligned antiparallel. As the external magnetic field is increased, the domain wall will

begin to propagate along the length of the material, increasing the size of the parallel aligned domain, and decreasing the size of the antiparallel aligned domain. But, since the saturation magnetization of the defect sites is higher than the surrounding material, the domain wall will be pinned at these sites, because the external magnetic field is not strong enough to change the magnetization of the defect sites.

Simulations were run with various pinning strengths, however, when smaller pinning strengths were used, the defect sites are not strong enough to pin the motion of the domain wall, and the domain wall freely propagates through the material. The defect site pinning strengths used were unrealistically large (greater than 10x the regular anisotropy constant), in order to pin the domain wall. The fact that small pinning strengths will not pin the domain wall properly is due to the small-scale nature of micromagnetic simulations. Edge effects begin to influence the energetics of the magnetic system at such small geometries. Any increase in the size of the sample within a simulation, exponentially increases the computational time needed to run the simulation. This limits the practical size of a sample within the micromagnetic simulator. Therefore, the maximum sample size is small – between 500 and 1000 nm wide, 2000 nm long, and 10 nm thick. Although the defect pinning strengths used in these simulations are unrealistic, the results are still highly relevant and informative.

Simulation Results

Explanation of Domain Wall Propagation

Figure 3-2 shows 3 stages of domain wall propagation: low field, medium field, and high field. Under low field, the domain wall exhibits small parabolic bowing with the edges pinned by the defect sites. Under medium field, the domain wall shows large bowing. The domain wall has

linear regions towards the sides of the material, with a parabolic bowing at the forefront of the domain wall. At high field, the domain wall is depinned from the defect sites, and the system seeks to equilibrate by magnetizing the entire sample in the same direction.

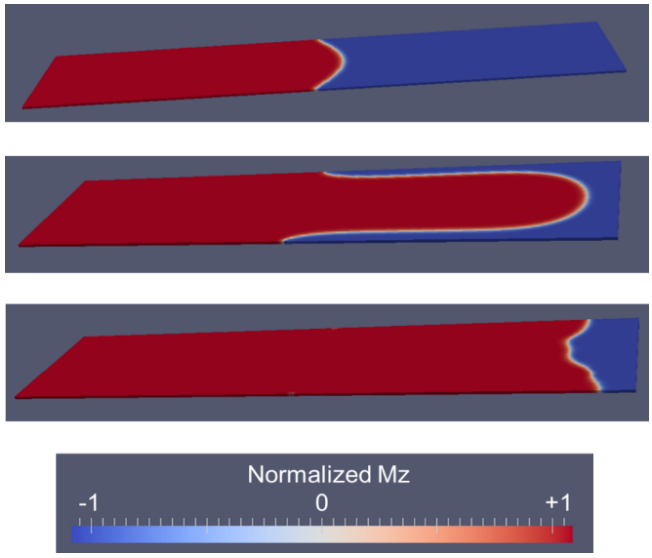

Figure 3-2. Three stages of domain wall propagation. Rendered using ParaView

The displacement of the domain wall is calculated by taking the distance between the forefront of the bowing domain wall, and its initial position. Figure 3-3 domain wall displacement versus external magnetic field for three different defect distances. As defect distance increases, it would be expected that the domain wall displacement will increase faster than for closer defects. Figure 3-3 proves that this is indeed the case. This can be understood by a simple rubber band analogy. The domain wall can be thought of as a rubber band, and the external magnetic field can be thought of as a force pulling on the rubber band. If the two edges of the rubber band are pinned, the rubber band will bow outwards upon application of a force. A shorter rubber band will require more force to move the same amount of distance, likewise with a domain wall with defect pinning sites.

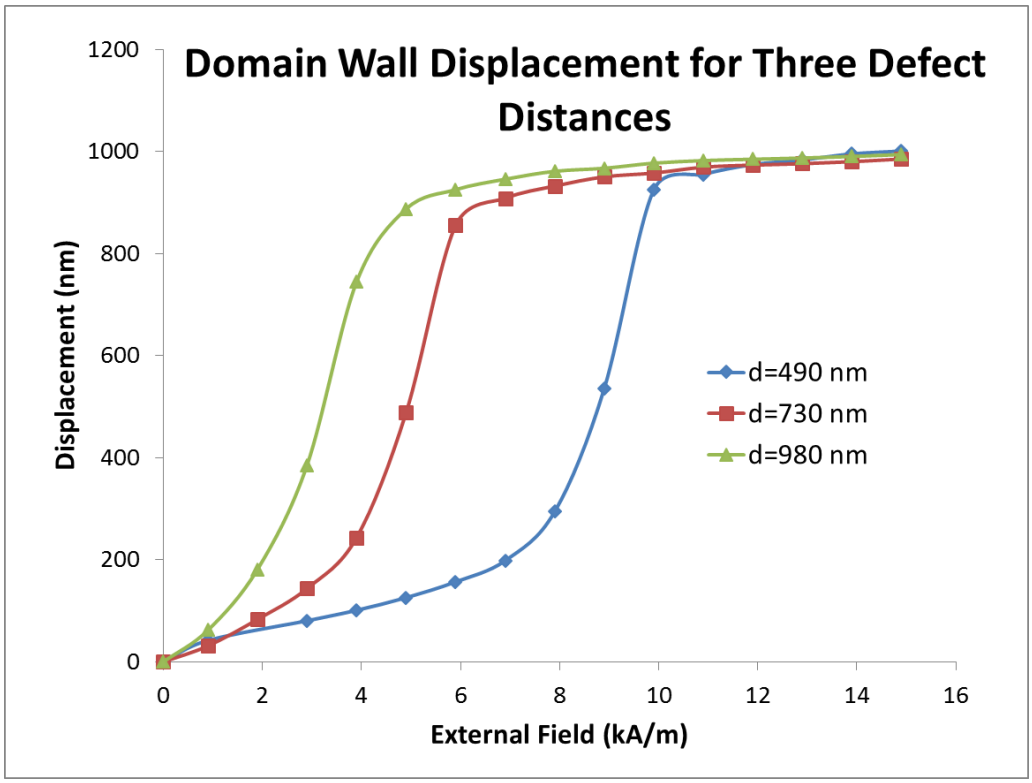

Figure 3-3. Domain wall displacement for three defect distances. Three different regions can be identified: a low field region (< kA/m), a medium field region (2-8 kA/m) and a high field region (> 8kA/m)

The domain wall position was extracted from simulation data using visualization software called ParaView. The initial domain wall position was taken as the zero point. Then, the midpoint of the domain wall was found by locating the area with zero magnetization, halfway between the width of the sample, since the domain wall is an area of zero magnetization. The zero point position was subtracted from the position of the midpoint of the domain wall to obtain a domain wall displacement value. Figure 3-3 reveals three regions of domain wall propagation: an initial region, between 0 and 2 kA/m, where domain wall displacement increases at a slow rate with external field, an intermediate region, between 2 and 4-8 kA/m, where displacement exponentially increases with external field, and a final region, between 4-8 and 16 kA/m, in

which the displacement plateaus. The intermediate region begins at different stages for different defect distances. The intermediate region begins earlier for higher distance between pinning sites, which is consistent with the rubber band analogy previously described. The plateau region is independent of distance between defect sites. In order to understand what is causing these various regions, an examination of the competing energy terms is needed.

Figure 3-4 shows the exchange field energy, the Zeeman energy, and the stray field energy, plotted as a function of external field for a pinning site distance of 490 nanometers. All the energy terms were normalized to the maximum stray field energy density $\frac{\mu_0}{2} M_s^2$. The anisotropy energy is omitted from this plot. It does not play a significant role, because all magnetic moments are aligned along the easy axis, except for the moments in the domain wall. The anisotropy energy therefor only changes when the length of the domain wall changes, and this number is small compared to the exchange and demagnetization energy. The stray field energy term dominates over the other energy terms, and plays the most significant role in determining the energetics of the system while it goes through the previously mentioned transition periods.

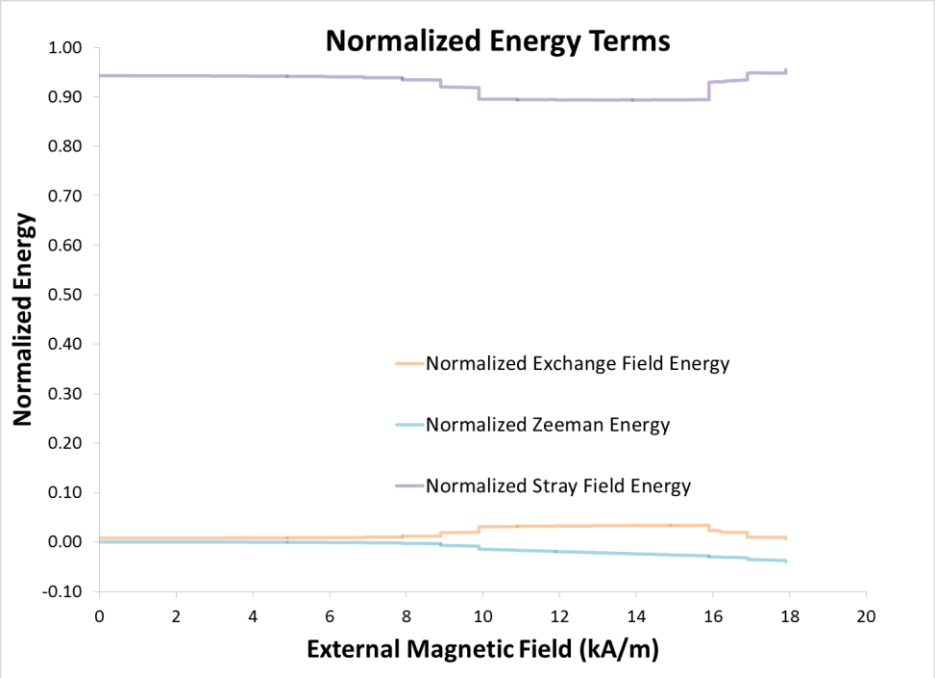

Figure 3-4. Exchange field energy, Zeeman energy, and stray field energy, normalized to the maximum demagnetization energy.

Two competing factors within the stray field energy cause the transition from a small bowing to a large bowing in the domain wall shape. First, the stray field energy seeks to have two equally sized and oppositely aligned domains, under no application of an external field. This is the case of Figure 2-1. As an external field is applied, the stray field energy will still prefer to have two oppositely aligned domains, but it will now be more energetically favorable for one of the domains to be larger, with magnetization along the external magnetic field direction than the other. In response, the domain wall would propagate. However, with two pinning sites, the domain wall cannot propagate as a whole, and so it begins to bow outwards.

There is, however, a favorable energy gain when the domain wall bows outwards. A parabolic domain wall is longer in length than a linear domain wall. An increase in the length of a domain wall, reduces the distance that magnetic field lines travel between oppositely aligned magnetic domains, and increases the magnetic field line density. This is illustrated in Figure 3-5a.

Imagine the infinite wandering domain wall (see Figure 3-5b) within a material. The stray field energy would approach a minimum, as the magnetic field lines created by the material would immediately close off, since an oppositely aligned domain would be so close, thereby lowering the energy of the system.

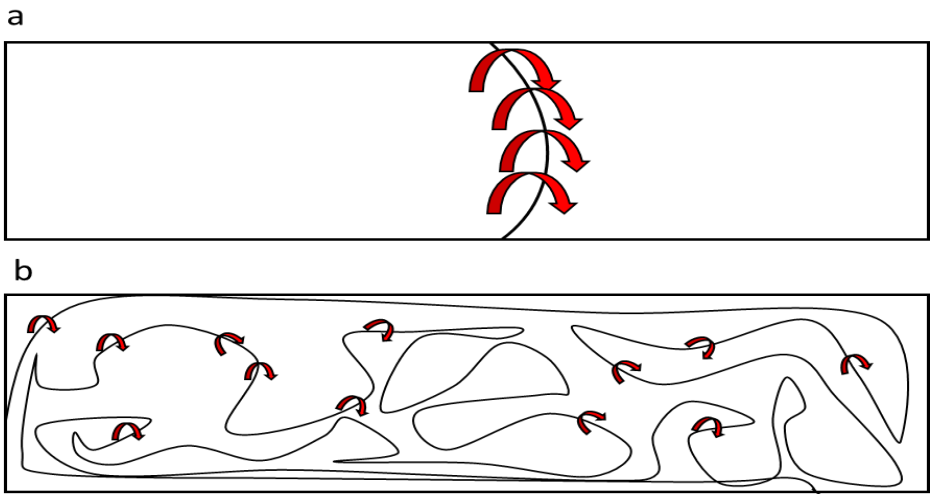

Figure 3-5. A parabolic domain wall (a) showing magnetic field lines, and a semi-infinite domain wall (b) showing a high density of magnetic field lines.

Relationship Between Anisotropy Energy and Domain Wall Length

Anisotropy energy is the energy gained in the system, when a magnetic moment is aligned parallel to the preferred axis, in this case, out-of-the-plane. As a domain wall deflects and thus lengthens, more magnetic moments are aligned in the plane. This causes an increase in anisotropy energy. Thus changes in the anisotropy energy directly reflect the domain wall length. As the external magnetic field increases, the domain wall deflects more, further increasing the anisotropy energy. Figure 3-6 shows anisotropy energy plotted versus domain wall displacement. The relationship is linear, except for a small region at small displacements of the domain wall. This is related to the shape of the domain wall. At small fields, the domain wall is parabolic, but the longer the domain wall gets, the more energetically favorable it is to become linear. This fact has useful possibilities, as it would now be possible to measure domain wall bowing length in a real material, if the energetics of the system are known.

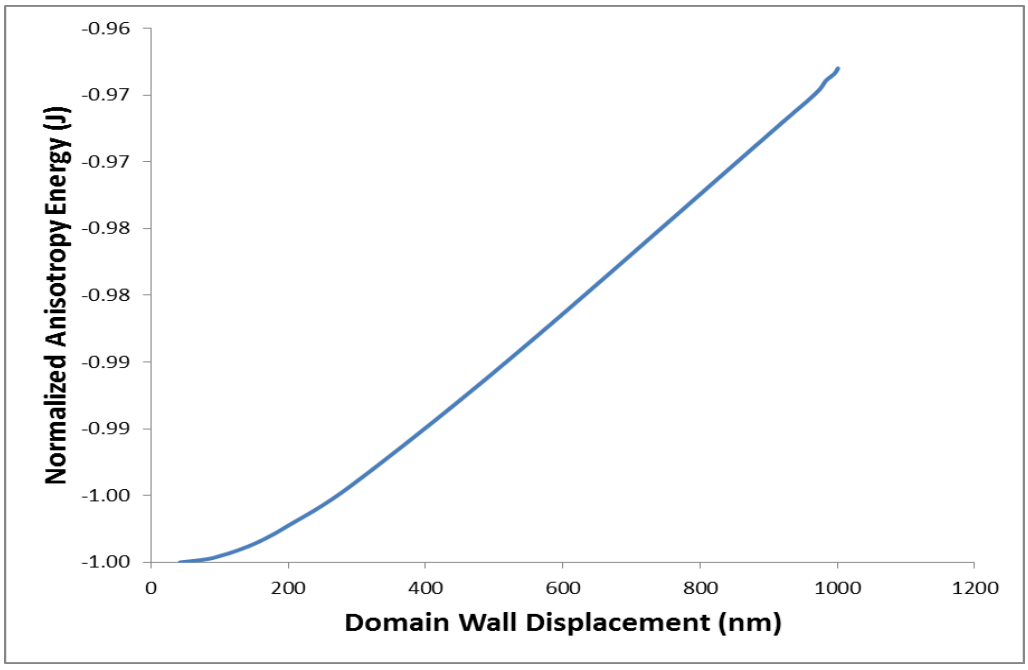

Figure 3-6. Anisotropy energy as a function of domain wall displacement. Information about a materials anisotropy energy response with respect to domain wall displacement could be used to calculate the domain wall displacement of a separate material system.

Conclusions

A hysteresis curve was calculated for CoPt. Initial studies of domain wall movement were conducted for the magnetic system of CoPt. Several things were discovered. As expected, a larger distance between pinning centers results in a more flexible domain wall. Three different regimes of domain wall displacement were examined:

1. An initial regime under low external field, where there is minimal bowing of the domain wall.
2. A transition regime, in which the displacement of the domain wall increases rapidly, as two stray field energy interactions compete with one another.
3. A plateau regime, that stays constant independent of distance between pinning centers, prior to the depinning of the domain wall

These three regimes were explained and characterized based on the different energy contributions to the magnetic system.

Future Work

There are a variety of interesting problems left to investigate. Studying how domain wall movement is affected by current, rather than external magnetic field, is an important step towards making racetrack memory commercially viable. It would also be prudent to study pinned domain wall movement under an oscillating field or current. From this, one could discover a resonant frequency for a domain wall, and the energy stored within a domain wall.

.

REFERENCES

[1] "IBM 701 Tape Drive." [Online]. Available: http://www.columbia.edu/cu/computinghistory/701-tape.html. [Accessed: 08-Apr-2013].

[2] "History of Computers and Computing, Birth of the modern computer, The bases of digital computers, Magnetic Tape of Valdemar Poulsen and Fritz Pfleumer." [Online]. Available: http://history-computer.com/ModernComputer/Basis/tape.html. [Accessed: 08-Apr-2013].

[3] "The history of computer data storage, in pictures." [Online]. Available: http://royal.pingdom.com/2008/04/08/the-history-of-computer-data-storage-in-pictures/. [Accessed: 08-Apr-2013].

[4] IBM, "MIT Technology Review - Racetrack Memory." 2009.

[5] R. Engel-Herbert, "Micromagnetic study of self-organized magnetic nanostructures - DISSERTATION." 2006.

[6] A. L. Balk, "Nanoscale magnetization in ferromagnetic thin films." 2011.

[7] R. Boardman, "Computer simulation studies of magnetic nanostructures." 2005.

[8] Landau and Lifshitz, "On the theory of the dispersion of magnetic permeability in ferromagnetic bodies." Physikalische Zeitschrift Sowjetunion,, 1935.

[9] J. A. Aboaf, S. R. Herd, and E. Klokholm, "Magnetic Properties and Structure of Cobalt-Platinum Thin Films." 1983.

[10] D. Alloyeau, "STEM nanodiffraction technique for structural analysis of CoPt nanoparticles." 2008.

ACADEMIC VITA

Zach Johnson

301 Cheswold Ct, Chesterbrook, PA, zjtennis@gmail.com

Education

B.A. or B.S., Materials Science and Engineering, 2013, The Pennsylvania State University,

University Park, PA

Schreyer Honors College Scholar

Dean's List Fall '09, '10, '11, '12 Spring '10, '11, '12

Professional Presentations

Summer Internship Report, PPG Industries,

Pittsburgh, PA,

September, 2013

Publications and Papers

Zha, Y., Disabb-Miller, M., Johnson, Z. D., Hickner, M., & Tew, G. (2012). Metal Cation-Based Anion Exchange Membranes. *Journal of the American Chemical Society*.